Electronic Supplementary Information (ESI)

One-pot synthesis of carbon-coated Ni_5P_4 nanoparticles and CoP nanorods for high-rate and high-stability lithium-ion batteries

Jun Jiang, [a,b,c,d] Chunde Wang,[a,b,c,d] Wei Li,[a,b,c,d] Qing Yang*,[a,b,c,d]

[a] *Hefei National Laboratory of Physical Sciences at the Microscale (HFNL), University of Science and Technology of China (USTC), Hefei 230026, Anhui, P. R. China.*

[b] *Department of Chemistry, USTC, Hefei 230026, Anhui, P. R. China.*

[c] *Laboratory of Nanomaterials for Energy Conversion (LNEC), USTC, Hefei 230026, Anhui, P. R. China.*

[d] *Synergetic Innovation Center of Quantum Information & Quantum Physics, USTC, Hefei 230026, Anhui, P. R. China.*

* *Corresponding author. E-mail: qyoung@ustc.edu.cn; Fax: +86-551-63606266; Tel: +86-551-63600243.*

1. EDX spectra for the as-prepared Ni_5P_4@C nanoparticles and CoP@C nanorods.

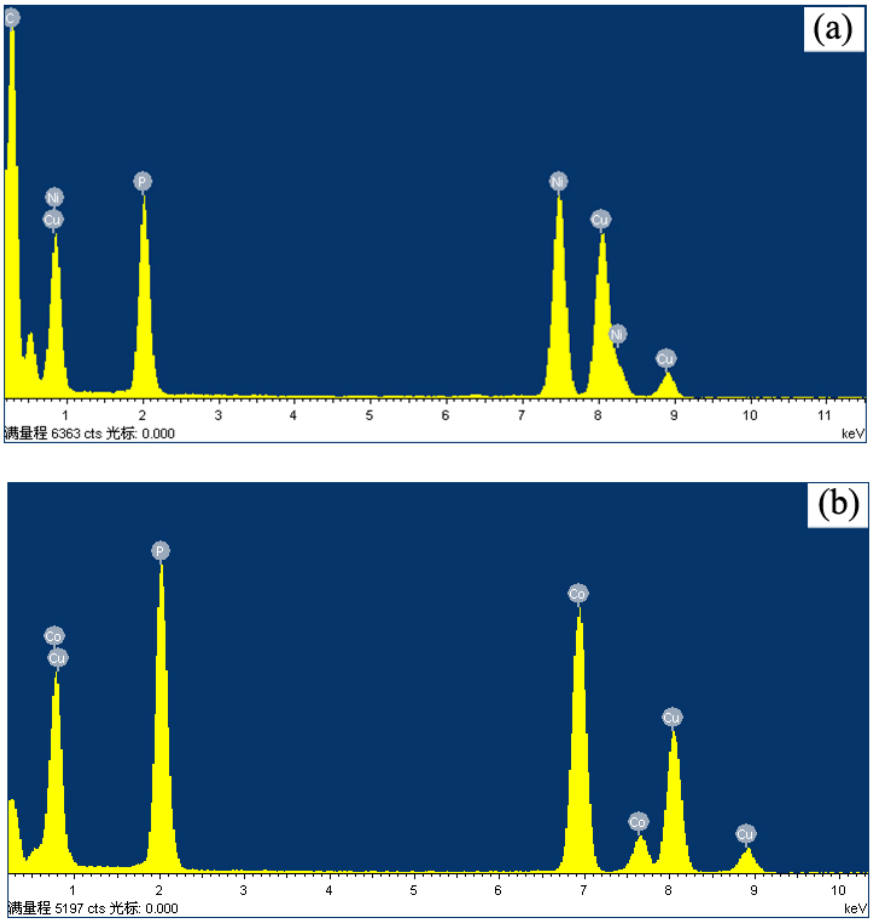

Fig. S1. (a) EDX spectra for the as-prepared Ni_5P_4@C nanoparticles, and (b) EDX spectra for the as-prepared CoP@C nanorods. The signal of Cu arises from the TEM grids.

2. Table S1. C, H and N contents of the as-prepared Ni_5P_4@C and CoP@C nanocomposites.

Sample	**C-content (wt. %)**	**H-content (wt. %)**	**N-content (wt. %)**
Ni_5P_4@C	18.65	1.24	0.07
CoP@C	9.72	1.70	0.08

3. XPS for the as-prepared Ni_5P_4@C nanoparticles.

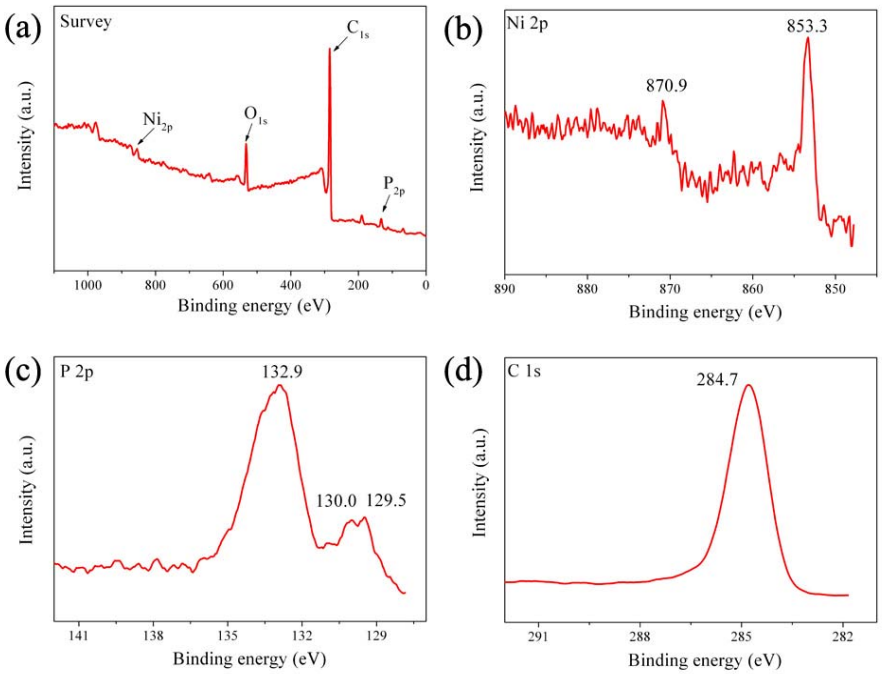

Fig. S2. (a) Survey, (b) Ni 2p, (c) P 2p and (d) C 1s XPS spectra collected for Ni_5P_4@C nanoparticles.

4. XPS for the as-prepared CoP@C nanorods.

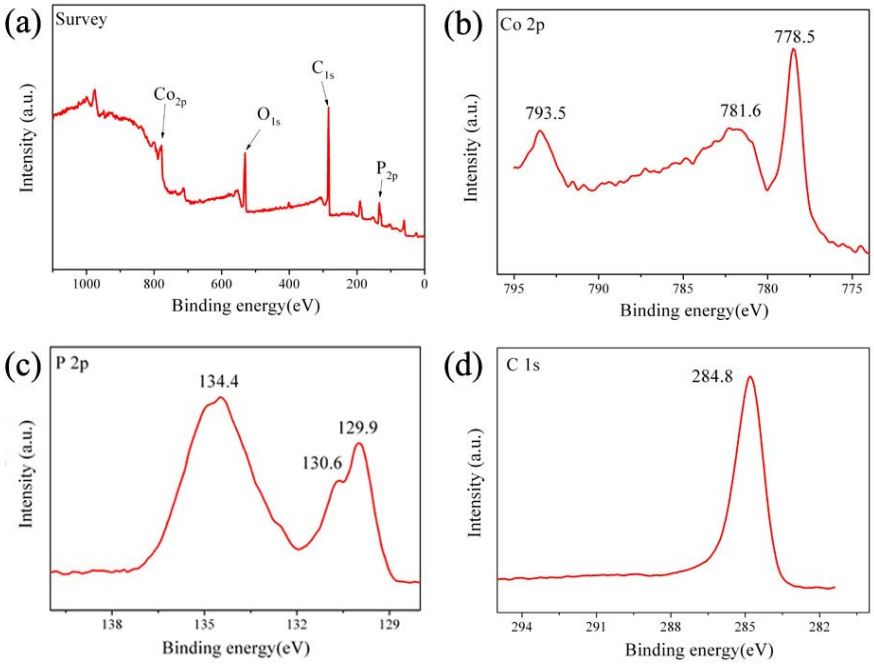

Fig. S3. (a) Survey, (b) Co 2p, (c) P 2p and (d) C 1s XPS spectra collected for CoP@C nanorods.

5. Cyclic voltammetries of the Ni_5P_4@C nanoparticles and CoP@C nanorods.

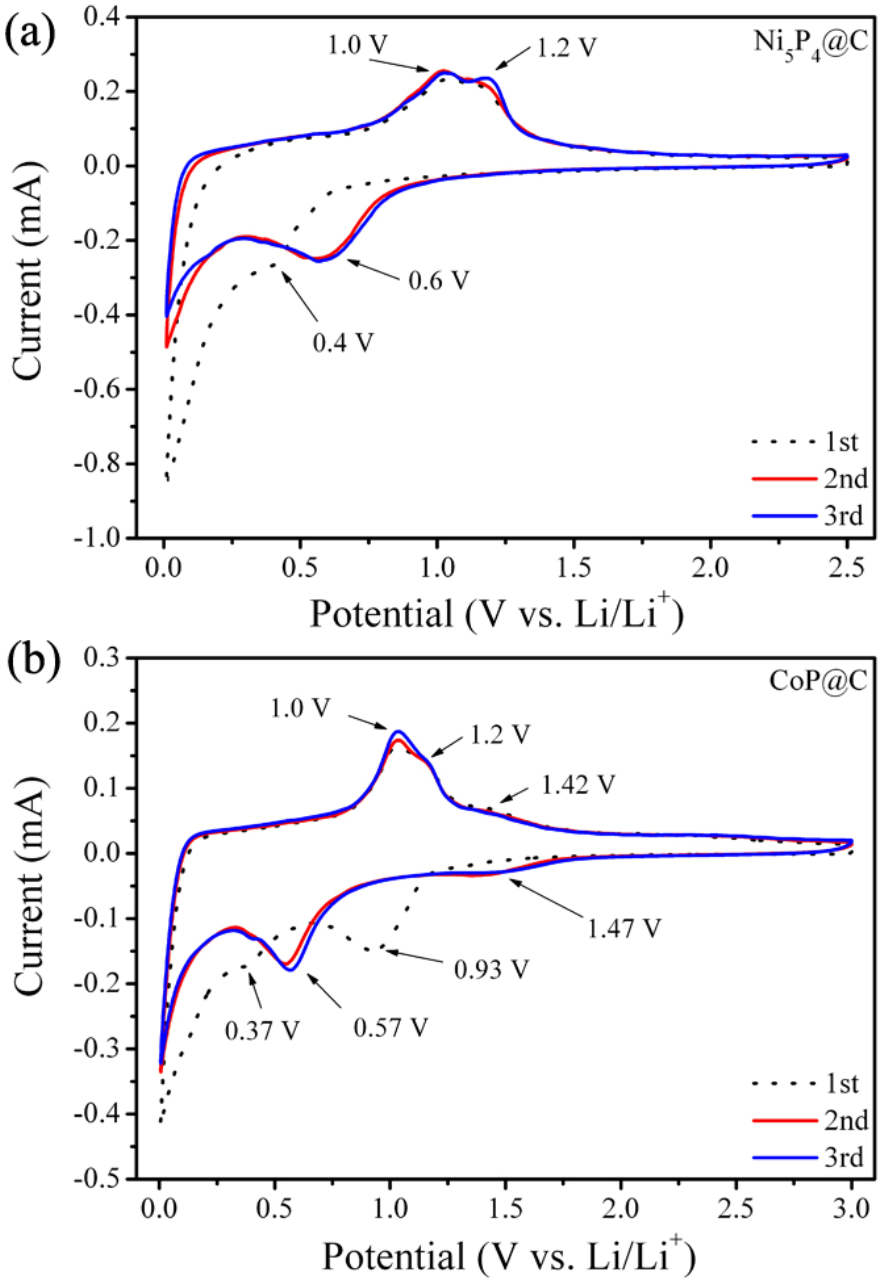

Fig. S4. (a) Cyclic voltammetries of the Ni_5P_4@C nanoparticles between 0.01 and 2.5 V at a scan rate of 0.1 mV s^{-1} for the 1st, 2nd and 3rd cycles, and (b) cyclic voltammetries of the CoP@C nanorods between 0.01 and 3.0 V at a scan rate of 0.1 mV s^{-1} for the 1st, 2nd and 3rd cycles.

6. Table S2. Comparison the as-prepared Ni_5P_4@C nanoparticles and CoP@C nanorods with previously reported transition-metal phosphide (TMP) structures.

Material	**Rate**	**Reversible capacity based on the total mass of MP@C/mA h g^{-1}**	**Reversible capacity based on the mass of MP/mA h g^{-1}**	**Ref.**
Ni_5P_4@C NPs	0.2C 1C 5C	490/100th cycle 370/200th cycle 339	612/100th cycle 462/200th cycle 424	This work
Ni_5P_4/C MPs	0.1C 3C	- -	644/50th cycle 357	16
CoP@C NRs	0.2C 1C 5C	579/100th cycle 469/200th cyce 340	654/100th cycle 530/200th cycle 384	This work
CoP@C NPs	0.2C 1C 5C	- - -	630/100th cycle 352 256	18

7. The phase stability of the Ni_5P_4@C nanoparticles and CoP@C nanorods at high temperature.

In order to test the phase stability of the as-prepared products, we load the as-prepared products in the sealed quartz tube and then annealing at 600 ^oC for 2h.

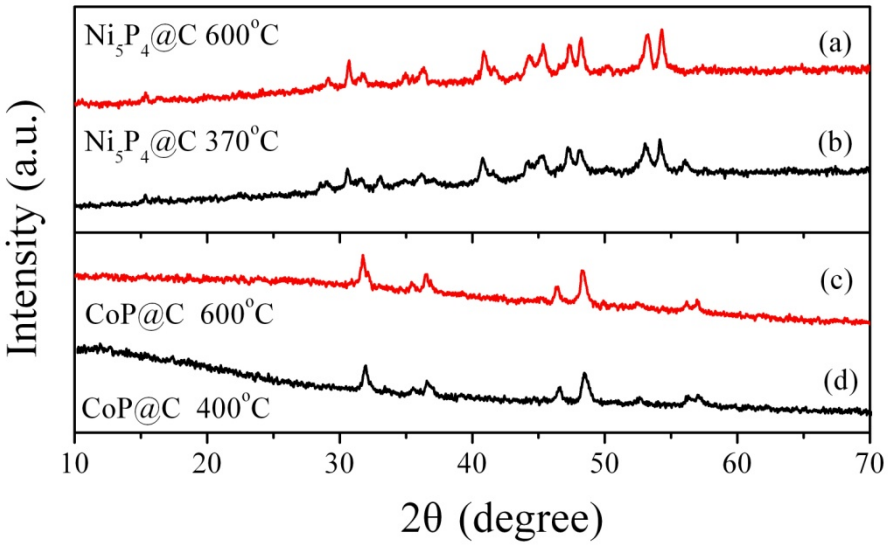

Fig. S5. XRD of the Ni_5P_4@C and CoP@C nanocomposites before/after annealing. (a) Ni_5P_4@C at 600 ^oC, (b) Ni_5P_4@C at 370 ^oC, and (c) CoP@C at 600 ^oC, (d) CoP@C at 400 ^oC.

8. Electrochemical performance of the Ni_5P_4@C nanoparticles and CoP@C nanorods in the full LIB cell.

We assemble the full LIB cell with the as-prepared products as anode and commercial $LiCoO_2$ as cathode. The loading mass of the products and $LiCoO_2$ on the electrode is ~0.5 mg and ~5.0 mg, respectively. Assuming a stable capacity delivery of 150 mA h g^{-1} for the $LiCoO_2$ cathode,[S1] the anode electrode capacity is less than the cathode electrode capacity in the cell, so the capacity in the full LIB is limited by the anode material. Hence the capacity and current density in this work is based on the mass of anode materials. With the potential between 1.5 V and 3.6 V and the current density at 0.2C, the Ni_5P_4@C-$LiCoO_2$ full cell shows a discharge voltage of ~3.0 V, and the charge capacity and dicharge capacity is ~510 mA h g^{-1} and ~380 mA h g^{-1}, respectively. With the same potential range and current density, the CoP@C-$LiCoO_2$ full cell shows a discharge voltage of ~3.0 V, and the charge capacity and dicharge capacity is ~500 mA h g^{-1} and ~350 mA h g^{-1}, respectively.

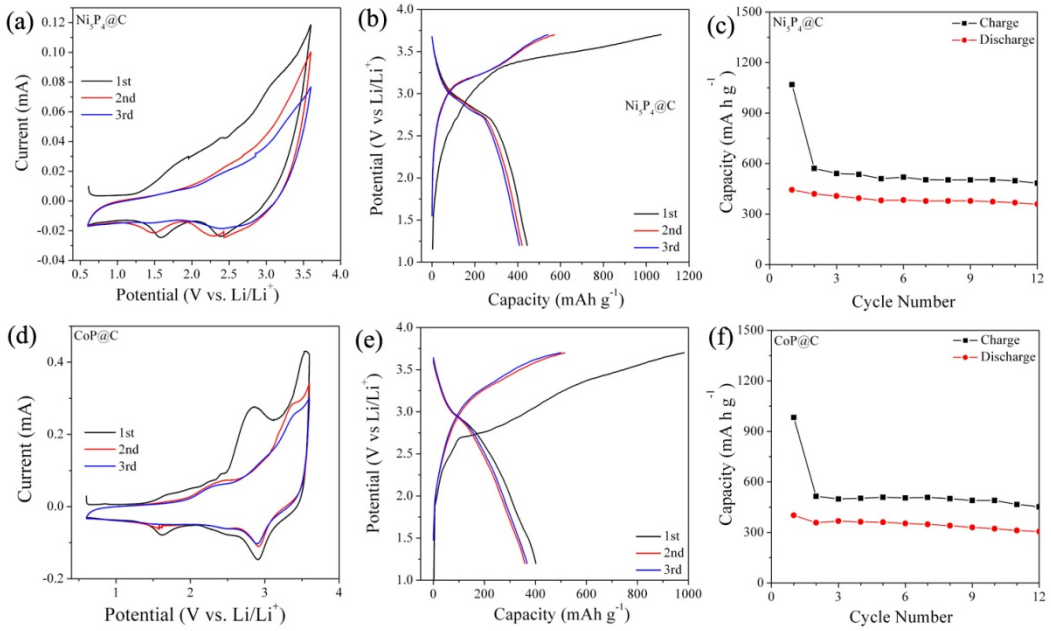

Fig. S6. (a) Cyclic voltammetries of the Ni_5P_4@C, (b) charge-discharge voltage profiles for the Ni_5P_4@C at 0.2C, (c) cycle performance of the Ni_5P_4@C at 0.2C, and (d) cyclic voltammetries of the CoP@C, (e) charge-discharge voltage profiles for the CoP@C, and (f) cycle performance of the CoP@C at 0.2C.

9. TEM images of the Ni_5P_4@C nanoparticles and CoP@C nanorods after cycling at 0.2C.

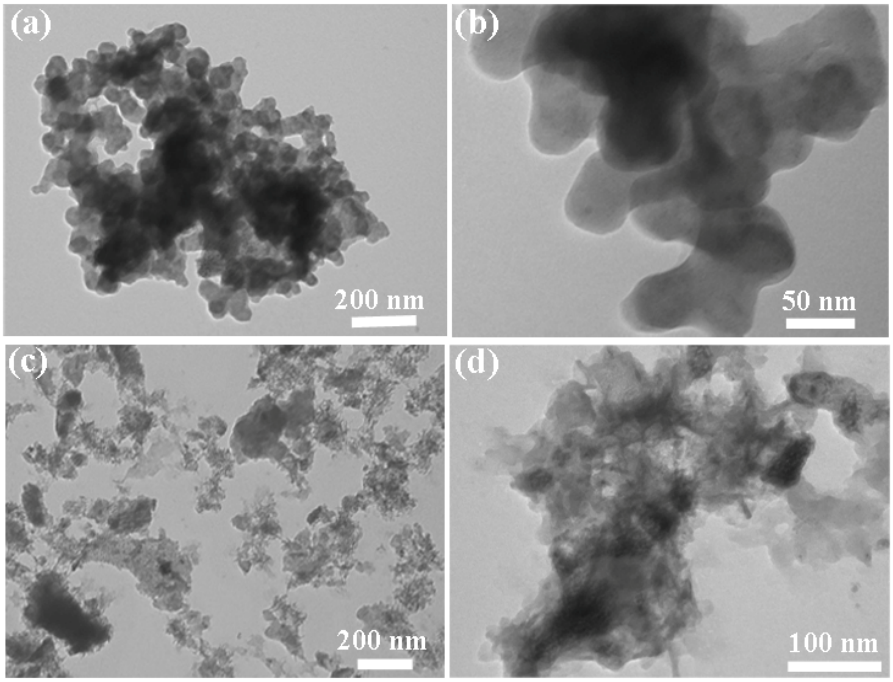

Fig. S7. (a), (b) TEM images of Ni_5P_4@C nanoparticles after 100 cycles at 0.2C in the cell, and (c), (d) TEM images of CoP@C nanorods after 100 cycles at 0.2C in the cell.

10. Synthesis and characterization of NiP_2@C microsphere.

Through increasing the molar ratio of the $Ni(acac)_2$ and PPh_3 to 1:10, improving the reaction temperature to 400 ^oC and even extending the reaction time to 5h, we try to synthesize the phase of NiP_2. As shown in Fig. S8, the major peaks can be indexed to cubic NiP_2 (73-0436), but several negligible peaks located at 15°, 30°, 53° and 54° suggest the co-existence of slight Ni_5P_4 impurity phase in the products.

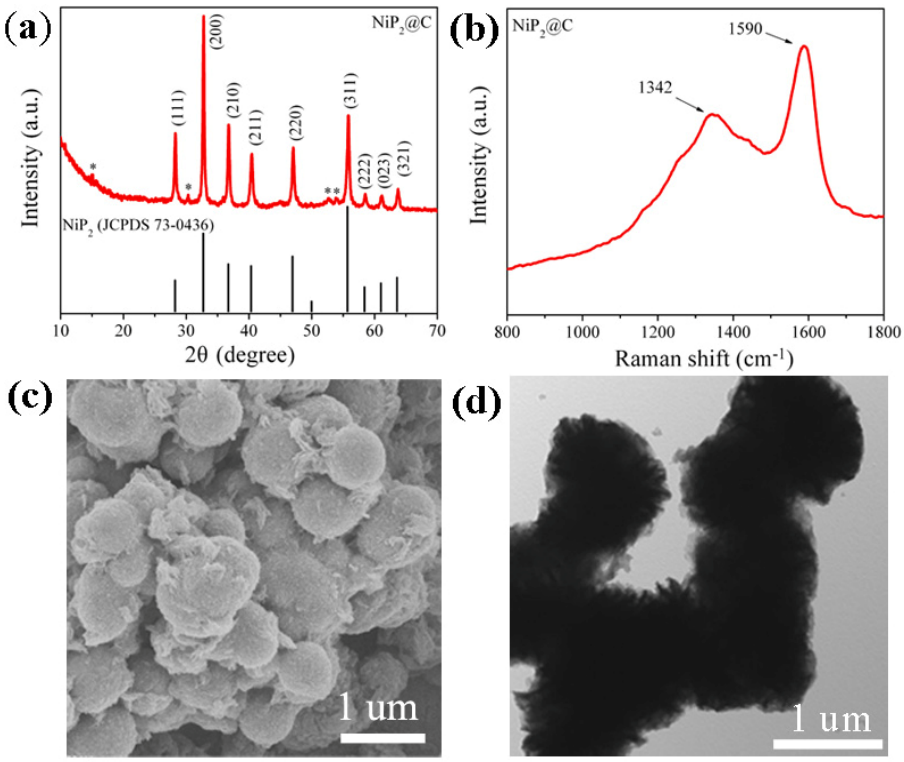

Fig. S8. (a) XRD, (b) Raman spectra, (c) SEM image and (d) TEM image of the as-prepared NiP_2@C composites.

Reference

S1. J. Liang, X. Li, Z. Hou, T. Zhang, Y. Zhu, X. Yan and Y. Qian, *Chem. Mater.* 2015, **27**, 4156-4164.